Journal of the Korean Nuclear Society
Volume 31, Number 2, pp.214~225, April 1999

Flexural Vibration of Clamped and Simply Supported Sectorial Plates with Combinations of Simply Supported and Free Radial Edges

Bong-Koo Han and Joo-Woo, Kim
Seoul National University of Technology
172 Kongneung-dong, Nowon-ku, Seoul 139-743, Korea
bkhan@duck.snut.ac.kr

(Received September 8, 1998)

Abstract

An accurate method is presented for flexural vibrations of sectorial plates having simply supported-free and free-free radial edges, when the circular edge is either clamped or simply supported. The classical Ritz method is employed with two sets of admissible functions assumed for the transverse vibratory displacements. These sets consist of : (1) mathematically complete algebraic-trigonometric polynomials which gurantee convergence to exact frequencies as sufficient terms are retained, and (2) corner functions which account for the bending moment singularities at re-entrant corner of the radial edges having arbitrary edge conditions. Accurate (at least four significant figures) frequencies and normalized contours of the transverse vibratory displacement are presented for the spectra of corner angles [90°, 180° (semi-circular), 270°, 300°, 330°, 350°, 355°, 360° (complete circular)] causing a re-entrant corner of the radial edges. Future solutions drawn from alternative numerical procedures and finite element techniques may be compared with these accurate results.

Key Words : ritz method, vibration, corner stress singularities, sectorial plate, bending, natural frequencies, mode shapes

1. Introduction

Accumulated in the literature for nearly two centuries are approximately 200 technical publications explaining the free vibration characteristics of complete circular and annular plates with various support conditions along the circumferential boundaries or at interior points. Extensive narratives of a lot of work have been chronicled in a summarizing monograph [1] and a series of review articles [2], [3], [4]. The scope of previous work done for the sectorial plate (see Fig. 1), in comparison, is quite narrow. Several authors have offered approximate theoretical and experimental vibration data for thin sectorial and annular sector plates with various edge conditions on the circular and radial edges [5], [6], [7], [8]. Bapu Rao *et al.* [9] and Guruswamy and Yang

[10] proposed various Reissner sector plate finite element formulations for approximate vibration analysis of circular and annular sectorial plates. Cheung and Chan [11] offered a three dimensionally curved finite strip method for static and vibration analyses of thin and thick sectorial plates with arbitrary conditions on the circular and radial edges. Indeed, these investigations collectively provide a solid groundwork for gaining a proper perspective of the significance of the title problem in the vibration literature.

Exact solutions for frequencies and mode shapes have long been known to exist for sectorial plates having simply supported radial edges, with arbitrary boundary conditions along the circular edge [1]. However, it has been shown [12], [13] that such solutions are not applicable when the sector angle α exceeds 180° (forming a re-entrant corner, see Fig. 1). An exact solution for this situation involves non-integer order ordinary and modified Bessel functions of the first and second kinds, and particular relationships among the four constants of integration to satisfy the corner stress singularities properly.

In some recent papers incorporating corner stress singularity effects [14], [15], [16] accurate (five significant figures) frequencies and mode shapes were presented for sectorial plates with free circumferential edge and clamped or free radial edges, and for completely free circular plates with rigidly constrained or free V-notches.

The present work examines sectorial plates having either a clamped or simply supported circumferential edge, and two combinations of simply supported and free radial edges, including stress singularity effects at the sharp vertex corner (see Fig. 1). For a very small notch angle, $360° - \alpha$ (say, one degree or less), a constrained, hinged, or free radial crack ensues. A Ritz procedure is employed, which incorporates a complete set of admissible algebraic-trigonometric polynomials in

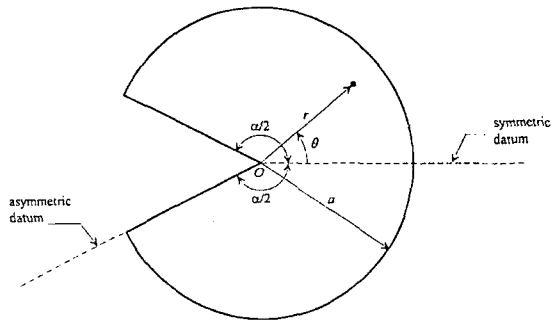

Fig. 1. Geometric Description of a Sectorial Plate

conjunction with an admissible set of corner functions that properly model the singular vibratory moments which exist at the vertices of corner angles (α) which exceed 180 degrees [17], [18]. The first set guarantees convergence to exact frequencies as sufficient terms are retained. The second set substantially accelerates the convergence of frequencies, which is demonstrated through an convergence study summarized herein. Accurate nondimensional frequencies are presented as the sector angle α is varied. To better understand the nature of the stress singularities existing in the title problem, normalized contour plots of the vibratory transverse displacements are studied for plates having corner angles α = 90°, 180° (semi-circular), 270°, 300°, 330°, 355°, and 360° (sharp radial crack).

2. Methodology

Consider the polar coordinates (r, θ) originating at the vertex of the sectorial plate of radius, a, shown in Figure 1. The transverse vibratory displacement w is defined in terms of these coordinates as follows :

$$w(r,\theta,t) = W(r,\theta)\sin\omega t \qquad (1)$$

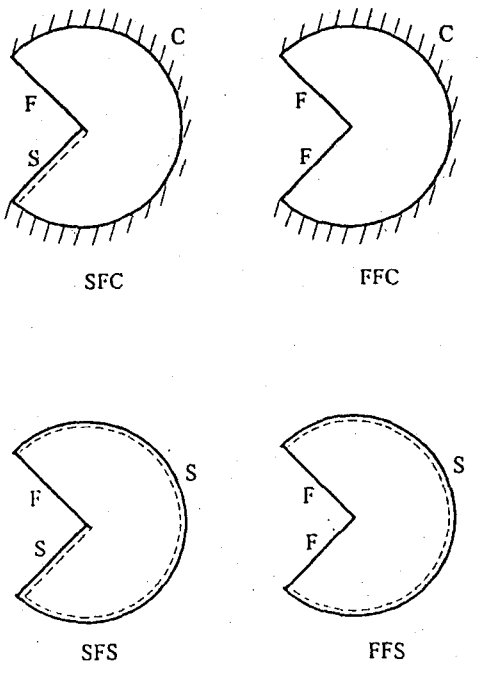

Fig. 2. Sectorial Plates with Various Combinations Clamped, Simply Supported and Free Edges

where t is time and w is the circular frequency of vibration. The boundary conditions for the various plates studied are identified according to the lettered edges shown in Fig. 2.

Displacement trial functions are assumed as the sum of two finite sets : $W=W_p+W_c$, where W_p are algebraic-trigonometric polynomials and are corner functions. The admissible polynomials for the *FFC*, and *FFS* plates are written as

$$W_p = g_1(r,\theta)\left(\sum_{m=0,2,4}^{M_1}\sum_{n=0,2,4}^{m} A_{mn} r^m \cos n\theta + \sum_{m=1,3,5}^{M_2}\sum_{n=1,3,5}^{m} A_{mn} r^m \cos n\theta\right) \quad (2)$$

for the symmetric vibration modes, and

$$W_p = g_1(r,\theta)\left(\sum_{m=2,4}^{M_3}\sum_{n=2,4}^{m} B_{mn} r^m \sin n\theta + \sum_{m=1,3,5}^{M_4}\sum_{n=1,3,5}^{m} B_{mn} r^m \sin n\theta\right) \quad (3)$$

for the antisymmetric modes, in which *M1*, *M2*, *M3*, and *M4* denote solution sizes, and for the

FFC plate: $g_1(r, \theta)=(a^2-r^2)^2$ (4a)

FFS plate: $g_1(r, \theta)=(a^2-r^2)$ (4b)

each of which is defined to satisfy the essential boundary conditions along the radial edges (see Fig. 1). Also indicated in Fig. 1 are datum lines utilized to define the symmetric and antisymmetric modes [Eqs. (2) and (3)]. No symmetry exists for the *SFC*, and *SFS* plates. Thus,

$$W_p = g_2(r,\theta)\left(\sum_{m=0,2,4}^{M_1}\sum_{n=0,2,4}^{m} A_{mn} r^m \cos n\theta + \sum_{m=1,3,5}^{M_2}\sum_{n=1,3,5}^{m} A_{mn} r^m \cos n\theta + \sum_{m=2,4}^{M_3}\sum_{n=2,4}^{m} B_{mn} r^m \sin n\theta + \sum_{m=1,3,5}^{M_4}\sum_{n=1,3,5}^{m} B_{mn} r^m \sin n\theta\right) \quad (5)$$

in which for the

SFC plate: $g_2(r, \theta)=(r/a)^2\,(\theta/\alpha)\,(a^2-r^2)^2$ (6a)

SFS plate: $g_2(r, \theta)=(r/a)^2\,(\theta/\alpha)\,(a^2-r^2)$ (6b)

In Eqs. (2), (3), and (5), A_{mn} and B_{mn} are arbitrary coefficients, and the values of m and n have been specially chosen to eliminate those terms which yield undesirable moment singularities at $r = 0$, and yet, preserve the mathematical completeness of the resulting series as sufficient terms are retained. Thus, convergence to the exact frequencies is guaranteed when the series is employed in the present Ritz procedure.

The displacement polynomial Eqs. (2), (3), and (5) should, in principle, yield accurate frequencies. However, the number of terms required may be computationally prohibitive. This problem is alleviated by augmentation of the displacement polynomial trial set with admissible corner

functions, which introduce the proper singular vibratory moments at the vertex corner formed by the radial edges (Fig. 1). The set of *corner functions* is taken as

$$W_c = G(r)\sum_{k=1}^{K} C_k W_{c_k}^{*} \tag{7}$$

where C_k are arbitrary coefficients, and $W^*_{c_k}$ are solutions of the fourth-order biharmonic, static equilibrium equation for bending of plates at acute corner angles [17].

$$W_{c_k}^{*}(r,\theta) = r^{\lambda_k+1}\left[a_k \sin(\lambda_k+1)\theta + b_k \cos(\lambda_k+1)\theta + c_k \sin(\lambda_k-1)\theta + d_k \cos(\lambda_k-1)\theta\right] \tag{8}$$

The essential boundary conditions along the radial edges $\theta = \pm\alpha/2$ may be simply supported [i.e., $W(r, \pm\alpha/2) = M_r(r, \pm\alpha/2) = 0$] or free [i.e., $V_r(r, \pm\alpha/2) = M_r(r, \pm\alpha/2) = 0$], where M_r and V_r are the usual radial moment and shear defined elsewhere [1]. These conditions are used in Eq. (8) to construct a set of algebraic equations from which the values λ_k are obtained as roots of the vanishing determinants.

For the *symmetric* modes of the *FFC* and *FFS* plates, $a_k = c_k = 0$ in Eq. (8), and satisfaction of the *free-free* (*F-F*) radial edge conditions results in the following characteristic equation for the λ_k,

$$\sin\lambda_k\alpha = -\frac{1-\nu}{3+\nu}\lambda_k \sin\alpha \tag{9}$$

The corresponding corner function for the *F-F* edge conditions is

$$W_{c_k}^{*}(r,\theta) = r^{\lambda_k+1}\left[\frac{\gamma_{1_k}\sin(\lambda_k-1)\alpha/2}{\gamma_{2_k}\sin(\lambda_k+1)\alpha/2}\cos(\lambda_k+1)\theta + \cos(\lambda_k-1)\theta\right] \tag{10a}$$

in which

$$\gamma_{1_k} = \lambda_k(\nu-1)+(3+\nu), \qquad \gamma_{2_k} = (\lambda_k+1)(\nu-1) \tag{10b}$$

Similarly, for the *antisymmetric* modes of the *FFC* and *FFS* plates, $b_k = d_k = 0$ in Eq. (8), and satisfaction of the *F-F* radial edge conditions results in the characteristic equation for the λ_k:

$$\sin\lambda_k\alpha = -\frac{1-\nu}{3+\nu}\lambda_k \sin\alpha \tag{11}$$

The corner functions used for the antisymmetric modes are analogous to those defined for the symmetric ones in Eqs. (10), except the cosine functions are changed to sine functions, and vice-versa.

Satisfaction of the *hinged-free* (*S-F*) radial edge conditions results in the following characteristic equation for the λ_k,

$$\sin 2\lambda_k\alpha = \frac{\nu-1}{3+\nu}\lambda_k \sin 2\alpha \tag{12}$$

The corresponding *S-F* corner function is

$$W_{c_k}^{*}(r,\theta) = r^{\lambda_k+1}\left[\sin(\lambda_k+1)\theta - \gamma_{1_k}\cos(\lambda_k+1)\theta - \gamma_{2_k}\sin(\lambda_k-1)\theta + \gamma_{3_k}\cos(\lambda_k-1)\theta\right] \tag{13}$$

where

$$\gamma_{1_k} = \frac{\sin(\lambda_k+1)\alpha/2}{\cos(\lambda_k+1)\alpha/2} \tag{14a}$$

$$\gamma_{2_k} = \frac{(\lambda_k+1)(\nu-1)}{\lambda_k(\nu-1)+(3+\nu)}\frac{\sin(\lambda_k+1)\alpha/2}{\sin(\lambda_k-1)\alpha/2} \tag{14b}$$

$$\gamma_{3_k} = \frac{(\lambda_k+1)(\nu-1)}{\lambda_k(\nu-1)+(3+\nu)}\frac{\sin(\lambda_k+1)\alpha/2}{\cos(\lambda_k-1)\alpha/2} \tag{14c}$$

For the *FFC* and *SFC* plates, the boundary function in Eq. (7), whereas for the *FFS* and *SFS* plates, $G(r)=(a^2-r^2)$. Some of the λ_k obtained from Eqs. (9), (11), and (12) may be complex numbers, and thus, result in complex corner functions. In such cases, both the real and

imaginary parts are used as independent functions in the present Ritz procedure outlined below. Although the same analytical procedure may be followed for *SSC* and *SSS* plates [12], an exact solution has been developed for cases when the two radial edges are simply supported [13].

In employing the Ritz method for free vibration problems, one has to construct the following frequency equations which, for the symmetric modes, are

$$\frac{\partial}{\partial A_{mn}}(V_{max}-T_{max})=0, \qquad \frac{\partial}{\partial C_k}(V_{max}-T_{max})=0 \quad (15)$$

and similarly for the antisymmetric modes, using B_{mn} in place of A_{mn}. In Eqs. (15), the maximum strain energy, V_{max}, in the plate due to bending in a vibratory cycle is

$$V_{max}=\frac{D}{2}\iint_A\left[(\chi_r+\chi_\theta)^2-2(1-\nu)\left(\chi_r\chi_\theta-\chi_{r\theta}^2\right)\right]dA \quad (16)$$

where $dA = rdrd\theta$, $D=Eh^3/12(1-\nu^2)$ is the flexural rigidity, h is the plate thickness, E is Young' s modulus, ν is Poisson' s ratio, and χ_r, χ_θ, and $\chi_{r\theta}$ are the maximum bending and twisting curvatures :

$$\chi_r=\frac{\partial^2 W}{\partial r^2}, \qquad \chi_\theta=\frac{1}{r}\frac{\partial W}{\partial r}+\frac{1}{r^2}\frac{\partial^2 W}{\partial\theta^2}, \qquad \chi_{r\theta}=\frac{\partial}{\partial r}\left(\frac{1}{r}\frac{\partial W}{\partial\theta}\right) \quad (17)$$

The maximum kinetic energy is

$$T_{max}=\frac{\rho\omega^2}{2}\iint_A W^2 dA \quad (18)$$

where ρ is the mass per unit area of the plate. The required area integrals in the dynamical energy Eqs. (16) and (18) are performed numerically, otherwise exact integrals are tractable when λ_k is real.

Substituting Eqs. (2) – (7), (10), (13), and (14) into (15) – (18) yields a set of homogeneous algebraic equations involving the coefficients A_{mn} (or B_{mn}) and C_k. The roots of the vanishing

Table 1. Convergence of Frequency Parameters $\omega a^2\sqrt{\rho/D}$ for a Sectorial Plate having Simply Supported-Free Radial Edges and Simply Supported Circumferential Edge (α = 330°)

Mode No.	No. of corner functions	Total number of terms in W_p			
		40	60	84	112
1	0	13.215	13.080	12.987	12.925
	1	12.986	12.835	12.729	12.658
	5	12.504	12.482	12.467	12.459
	10	12.454	12.451	12.449	12.448
	15	12.450	12.449	12.448	12.447
	20	12.449	12.448	12.448	12.447
2	0	16.399	16.061	15.850	15.700
	1	16.029	15.758	15.581	15.453
	5	14.195	14.176	14.165	14.159
	10	14.147	14.147	14.147	14.146
	15	14.147	14.147	14.146	14.146
	20	14.147	14.147	14.146	14.146
3	0	21.290	20.503	20.007	19.664
	1	17.436	17.314	17.254	17.224
	5	17.215	17.179	17.157	17.145
	10	17.137	17.134	17.132	17.131
	15	17.133	17.132	17.131	17.131
	20	17.132	17.131	17.131	17.131
4	0	25.435	24.929	24.585	24.347
	1	24.929	24.579	24.333	24.162
	5	23.503	23.484	23.471	23.465
	10	23.466	23.462	23.459	23.458
	15	23.460	23.459	23.458	23.457
	20	23.458	23.458	23.458	23.457
5	0	35.168	33.237	32.322	31.813
	1	35.147	33.234	32.321	31.810
	5	30.804	30.715	30.666	30.640
	10	30.628	30.619	30.614	30.612
	15	30.612	30.611	30.610	30.610
	20	30.610	30.610	30.610	30.610
6	0	39.573	39.145	38.925	38.801
	1	39.554	39.133	38.921	38.800
	5	38.606	38.567	38.555	38.549
	10	38.575	38.547	38.543	38.541
	15	38.546	38.542	38.540	38.540
	20	38.542	38.540	38.540	38.540

determinant of these equations are a set of eigenvalues, which are expressed in terms of the nondimensional frequency parameter $\omega a^2\sqrt{\rho/D}$ commonly used in the plate vibration literature. Eigenvectors involving the coefficients A_{mn} (or B_{mn}) and C_k are determined in the usual manner by substituting the eigenvalues back into the homogeneous equations. Normalized contours of the associated mode shapes may be depicted on a r-θ grid in the sector plate domain, once the eigenvectors are substituted into Eqs. (2), (3), (5), and (7).

3. Convergence Studies

Having outlined the Ritz procedure employed in the present analysis, it is now appropriate to address the important question of convergence rate of frequencies, as various numbers of algebraic-trigonometric polynomials and corner functions are retained. In this section, convergence studies are summarized for sectorial plates with a 30° notch angle (i.e., α = 330°). All of the frequency and mode shape data shown in the present and following sections are for materials having a Poisson's ratio (ν) equal to 0.3. Numerical calculations of all vibratory frequencies and mode shapes were performed on an IBM/RS-6000 970 powerserver with an IBM/RS-6000 340 workstation cluster using double precision (14 significant figure) arithmetic.

Consider the first six nondimensional frequencies $\omega a^2\sqrt{\rho/D}$ for the *SFS* (Table 1) sectorial plates (α=330°). Numerical results are shown as 40, 60, 84, and 112 polynomial terms are retained in Eqs. (2), (3), or (5), in conjunction with 0, 1, 5, 10, 15, and 20 corner functions employed in Eq. (7). In these cases a larger number of polynomial terms is required due to the absence of symmetry of edge conditions.

As indicated in Table 1, the lowest frequency mode of a *SFS* plate exhibits a slow upper bound monotonic decrease of $\omega a^2\sqrt{\rho/D}$ to an inaccurate value of 12.925, as the number of polynomial terms (W_p) is increased with no corner functions. That is, the polynomial series, albeit complete, is converging very slowly. An examination of the next five rows of data reveals that an accurate value to five significant figures is 12.447. Interestingly, a trial set consisting of a single corner function (corresponding to the lowest λ_k) along with a smaller number of 84 polynomial terms yields an upper bound $\omega a^2\sqrt{\rho/D}$ value of 12.729 which is slightly lower than the 12.925 value obtained with 112 polynomial terms and no corner functions. With larger trial sets of 84 polynomials and 10 corner functions, four significant figure convergence of the lowest frequency mode is achieved. One can clearly see that by adding the first 20 corner functions to as few as 40 polynomials yields the value of 12.449, which is exact to four significant figures. It should be noted that the *SFS* cases are the one of the most challenging convergence studies (with regard to the number of corner functions required) among the four problems analyzed here, and that the other boundary condition cases required fewer corner functions to achieve the proper convergence of frequencies.

4. Frequencies and Mode Shapes

Extensive convergence studies were performed to compile in Tables 2 and 3 the least upper bound frequency parameters $\omega a^2\sqrt{\rho/D}$ for the first six modes of sectorial plates with increasing sector angles α = 90°, 180°, 270°, 300°, 330°, 350°, 355°, and 360°. Listed in Table 2 are frequency parameters for sectorial plates having simply supported-free and free-free radial edge conditions along with a clamped circumferential edge (i.e.,

Table 2. Frequency Parameters $\omega a^2\sqrt{\rho/D}$ for Sectorial Plates Having various Radial Edge Conditions and Clamped Circumferential Edge

Case	α (degrees)	Mode No.					
		1	2	3	4	5	6
SFC	90	19.660	45.088	57.666	82.477	102.42	115.45
	180	19.185	26.103	40.054	56.078	56.853	69.434
	270	20.629	21.420	28.825	38.315	49.013	59.368
	300	20.002	21.475	26.724	34.992	44.241	54.366
	330	19.669	21.842	25.075	32.367	40.488	49.375
	350	19.622	22.018	24.146	30.903	38.402	46.594
	355	19.629	22.054	23.930	30.566	37.924	45.956
	360	19.646	22.112	23.726	30.241	37.461	45.341
FFC	90	7.5632	24.760*	31.991	56.561	67.925*	77.195
	180	8.6013	19.660*	28.857	36.329	45.088*	57.665*
	270	9.3280	18.814*	22.799	32.036*	37.029	42.016
	300	9.4879	18.847*	21.720	29.610*	36.634	39.031
	330	9.6137	18.972*	20.932	27.675*	34.638	38.378
	350	9.6806	19.096*	20.534	26.585*	33.148	38.392
	355	9.6955	19.131*	20.449	26.334*	32.795	38.406
	360	9.7094	19.167*	20.370	26.096*	32.457	38.421

*Antisymmetric modes

Table 3. Frequency Parameters $\omega a^2\sqrt{\rho/D}$ for Sectorial Plates Having Various Radial Edge Conditions and Simply Supported Circumferential Edge

Case	α (degrees)	Mode No.					
		1	2	3	4	5	6
SFC	90	12.498	34.872	45.608	68.868	86.609	98.448
	180	11.989	18.022	30.269	44.265	45.254	56.285
	270	13.358	13.672	20.368	28.696	38.228	47.212
	300	12.758	13.840	18.555	25.763	33.954	43.035
	330	12.447	14.146	17.131	23.457	30.610	38.540
	350	12.391	14.291	16.329	22.177	28.760	36.044
	355	12.393	14.321	16.144	21.883	28.337	35.474
	360	12.405	14.373	15.968	21.600	27.928	34.924
FFS	90	2.4426	17.167*	23.046	45.387	54.921*	63.235
	180	3.5149	12.498*	20.593	26.707	34.871*	45.608*
	270	4.1463	11.708*	15.264	23.221*	27.380	31.993
	300	4.2826	11.723*	14.319	21.089*	27.172	29.189
	330	4.3902	11.818*	13.626	19.392*	25.512	28.500
	350	4.4481	11.916*	13.274	18.441*	24.200	28.512
	355	4.4610	11.945*	13.198	18.223*	23.888	28.525
	360	4.4735	11.974*	13.129	18.015*	23.590	28.539

*Antisymmetric modes

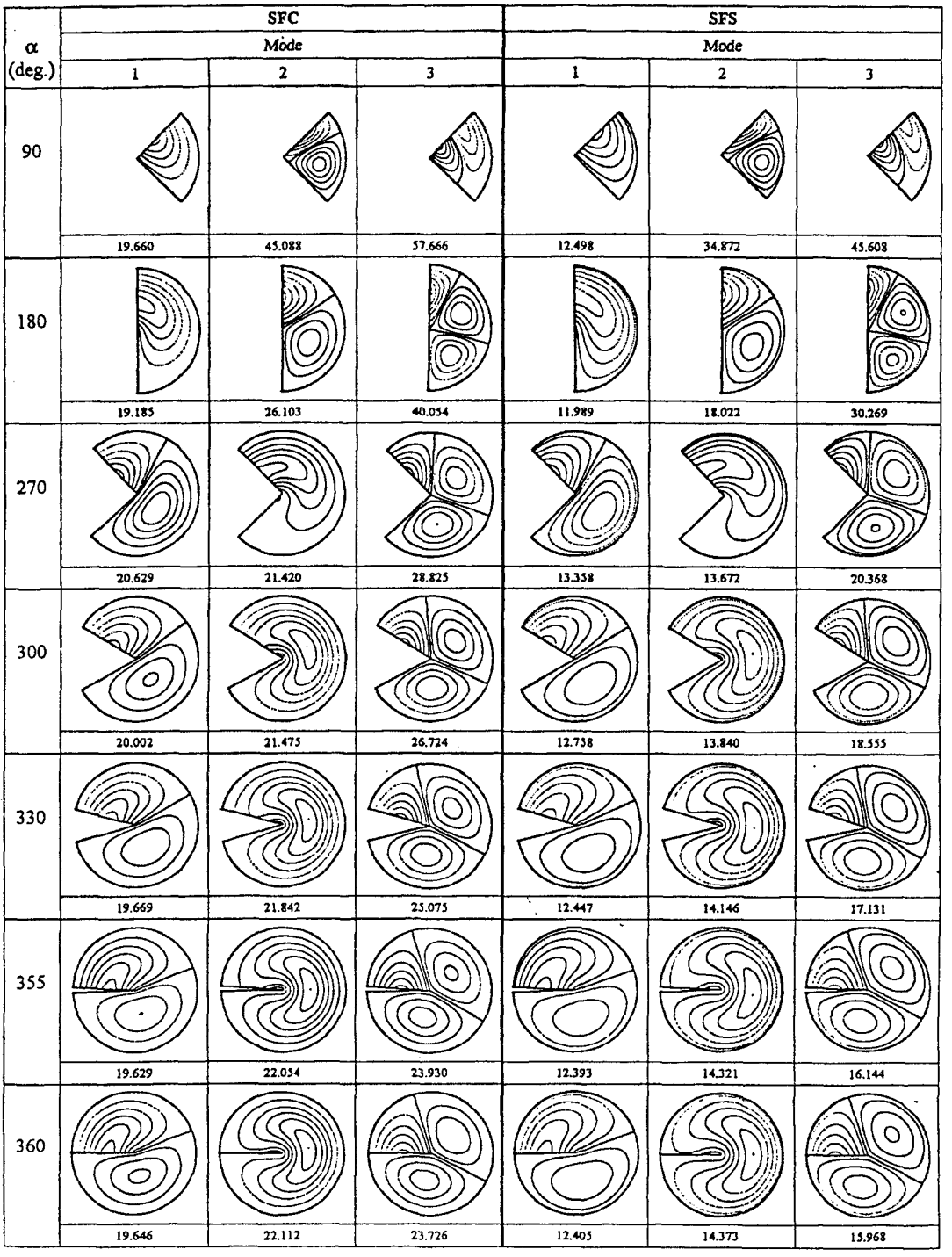

Fig. 3. Normalized Transverse Displacement Contours (W/W_{max}) for the First Three Modes of *SFC* and *SFS* Sectorial Plates

SFC and *FFC*), whereas shown in Table 3 are frequency data for plates with the same radial edge conditions and a simply supported circumferential edge (i.e., *SFS* and *FFS*). Plates having both radial edges simply supported are omitted, for accurate frequencies were presented by Huang *et al.* [13]. Frequency parameters corresponding to the antisymmetric modes are indicated by a superscript asterisk (*) as appropriate to the *FFS* and *FFC* plates. All frequency results are guaranteed upper bounds to exact values (typically accurate to the five significant figures shown in Tables 2 and 3). Hence, Tables 2 and 3 provide an accurate database of frequencies for sectorial plates having various edge conditions and notch angles against which future results using experimental or other numerical methods (such as finite element analysis) may be compared.

As can be expected, the frequency parameters of sectorial plates having a clamped circumferential edge are higher than those having a simply supported circumferential edge for all combinations of radial edge conditions. Generally speaking, it is clear that $\omega a^2\sqrt{\rho/D}$ decreases as the sector angle α increases. Slight exceptions to this trend is shown in the first and second modes of the *SFC* and *SFS* plates, the second and sixth modes of the *FFC* plate, and the second mode of the *FFS* plate, all of which exhibit a slight decrease, followed by a slight increase in $\omega a^2\sqrt{\rho/D}$ with decreasing α. However, a major exception to the trend occurs for the fundamental (i.e., lowest) frequencies of the *FFC* and *FFS* plates, which increase monotonically as α increases. In these cases the sole support of the plate is along its circular boundary, and the length of this support increases as α increases, which increases the stiffness of the system. The higher modes have radial node lines, which are equivalent to additional supports.

Shown in Figs. 3-4 are normalized displacement contours for the first three modes of sectorial plates (contours for the higher modes are not shown here for the sake of brevity) with various boundary conditions for α = 90°, 180°, 270°, 300°, 330°, 355°, and 360°. These contour plots are normalized with respect to the maximum transverse displacement component (i.e., $-1 \leq W/W_{max} \leq 1$, where the negative values of (W/W_{max} are depicted as dashed contour lines in Figs. 3 and 4, and the nondimensional frequencies shown correspond to the data listed in Tables 2 and 3). Contour lines are shown for W/W_{max} = $\pm$0.2, $\pm$0.4, $\pm$0.6, $\pm$0.8, $\pm$1. Nodal patterns of each mode are shown in Figs. 3 and 4 as darker contour lines of zero displacement (W/W_{max}=0) during vibratory motion.

The normalized displacement contours of the *FFC* and *FFS* plates are not substantially influenced by the decrease in notch angle from 90° to 5° (see Fig. 4). Given the absence of symmetry in the *SFC* and *SFS* displacement contours (see Fig. 3), their nodal patterns are rotated slightly in the clockwise direction in relation to the nodal patterns of the *FFC* and *FFS* plates, respectively. It is interesting to note that the fundamental mode shapes for the *SFC* and *SFS* plates with $\alpha \geq 270°$ have one nodal line, which is nearly radial, whereas the second mode shapes have none. Across the board in Figs. 3 and 4, the W/W_{max} contours and nodal patterns of the sectorial plates are only slightly changed by the clamped or simply supported circumferential edge conditions. As expected, the contour lines W/W_{max} = $\pm$0.2 occur closer to a simply supported circumferential edge than a clamped one, since in the latter both the normal displacement [$W(a,\theta)$] and the bending slope [$\partial W(a,\theta)/\partial r$] vanish.

5. Concluding Remarks

Highly accurate frequencies and mode shapes

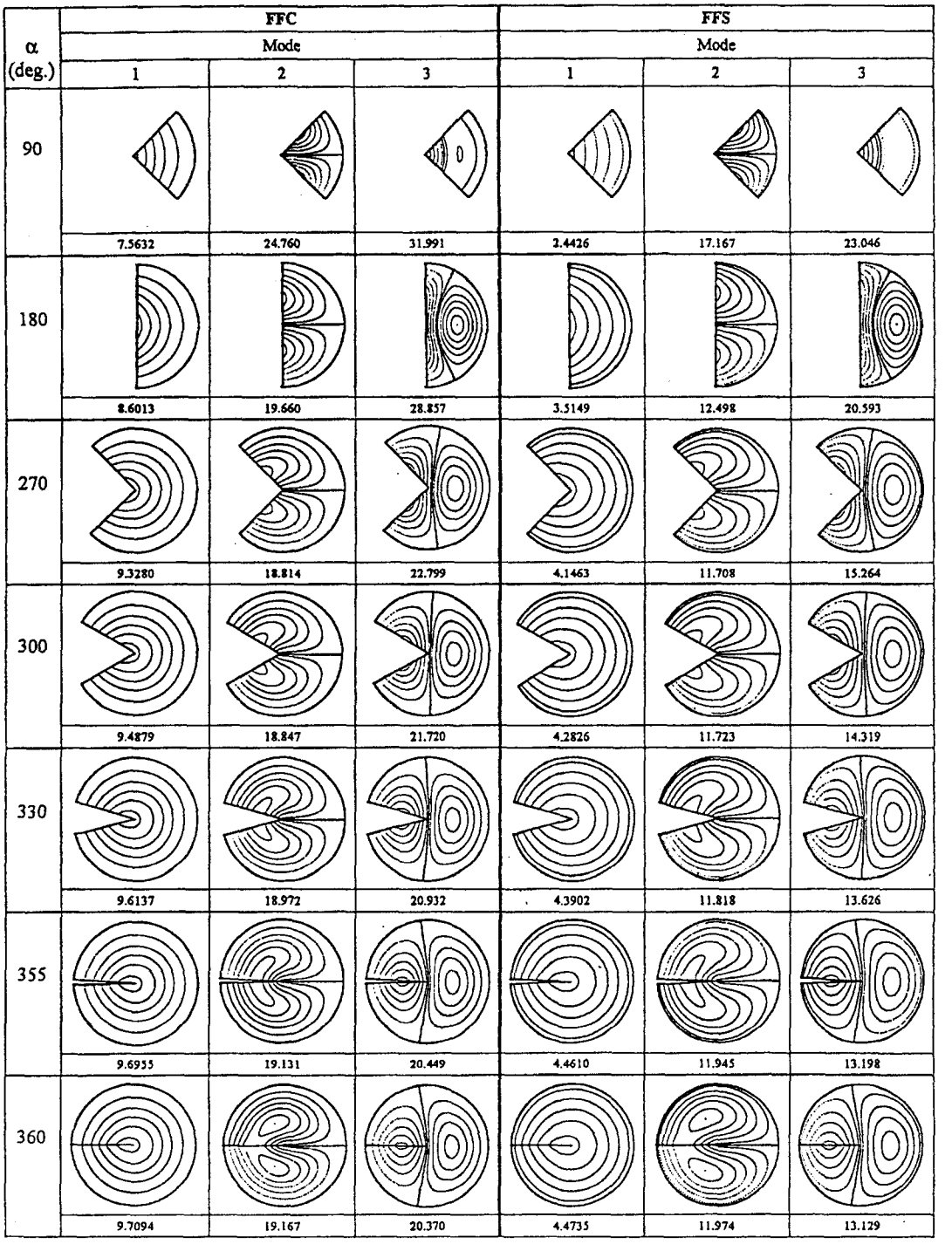

Fig. 4. Normalized Transverse Displacement Contours (W/W_{max}) for the First Three Modes of *FFC* and *FFS* Sectorial Plates

for sectorial plates with a clamped or simply supported circumferential edge and combinations of simply supported and free radial edges have been obtained using a Ritz procedure in conjunction with classical thin-plate theory. In this approximate procedure, the assumed transverse displacement of the plate constitutes a hybrid set of complete algebraic-trigonometric polynomials along with corner functions that account for singular bending moments at the vertices of acute corner angles.

Detailed numerical tables have been presented, showing the variations of nondimensional frequencies (accurate to at least five significant figures) over a spectra of corner angles α. No results were given for the *SSC* or *SSS* cases for they exist elsewhere [12], [13]. A primal conclusion explicating the title problem is that the large bending moment stresses in the neighborhood of the vertices of simply supported or free radial edges of vibrating sectorial plates do indeed significantly influence the frequencies.

The present variational Ritz approach is computationally effective for modeling the unbounded vibratory stresses, which exist at the sharp corners of constrained radial edges of sectorial plates. A point of methodological procedure is that investigators using continuum-based and discrete element-based formulation will have difficulty in calculating accurate solutions to the title problem unless they explicitly consider in the assumed displacement or stress fields the moment singularities at the sharp re-entrant corner ($\alpha > 180°$). The present method can be used to set up resonant responses for the plates having highly localized stresses. Such plates may be found as components of aircraft, machine, and civil engineering structures subject to cyclic loading. Most of all, the accurate vibration data presented here serves as benchmark values for comparison with data obtained using modern experimental and alternative theoretical approaches.

Acknowledgements

This paper was supported by the research fund of Seoul National University of Technology.

Referemces

1. Leissa, A. *W., Vibration of Plates, NASA SP-160.* Washington, D.C.: U.S. Government Printing Office, (1969) (Reprinted by The Acoustical Society of America, (1993).
2. Leissa, A. W., "Recent research in plate vibrations: classical theory," *The Shock and Vibration Digest*, Vol. 9, No. 10, pp. 13-24, (1977).
3. Leissa, A. W., "Plate vibration research, 1976-1980: classical theory," *The Shock and Vibration Digest*, Vol. 13, No. 9, pp. 11-22, (1981).
4. Leissa, A. W., "Recent studies in plate vibrations: 1981-1985, part I, classical theory," *The Shock and Vibration Digest*, Vol. 19, No. 2, pp. 11-18, (1987).
5. Bhattacharya, A. P. and Bhowmic, K. N., "Free vibration of a sectorial plate," *Journal of Sound and Vibration*, Vol. 41, No. 4, pp. 503-505, (1975).
6. Rubin, C., " Nodal circles and natural frequencies for the isotropic wedge," Journal of Sound and Vibration, Vol. 39, No. 4, pp. 523-526, (1975).
7. Maruyama, K. and Ichinomiya, O., "Experimental investigation of free vibrations of clamped sector plates," *Journal of Sound and Vibration*, Vol. 74, No. 4, pp. 563-573, (1981).
8. Kim, C. S., and Dickinson, S. M., "On the free, transverse vibration of annular and circular,

thin, sectorial plates subjected to certain complicating effects," *Journal of Sound and Vibration*, Vol. 134, pp. 407-421, (1989).

9. Bapu Rao, M. N., Guruswamy, P., and Sampath Kumaran, K. S., "Finite element analysis of thick annular and sector plates," *International Journal of Nuclear Engineering and Design*, Vol. 41, pp. 247-255, (1977).
10. Guruswamy, P. and Yang, T. Y., "A sector finite element for dynamic analysis of thick plates," *Journal of Sound and Vibration*, Vol. 62, pp. 505-516, (1979).
11. Cheung, M. S. and Chan, M. Y. T., "Static and dynamic analysis of thin and thick sectorial plates by finite strip method," *Computers and Structures*, Vol. 14, pp. 79-88, (1981).
12. Leissa, A. W., McGee, O. G., and Huang, C. S., "Vibration of sectorial plates having corner stress singularities," *ASME Journal of Applied Mechanics*, Vol. 60, pp. 134-140, (1993).
13. Huang, C. S., Leissa, A. W., and McGee, O. G., "Exact analytical solutions for the vibrations of sectorial plates with simply supported radial edges," *ASME Journal of Applied Mechanics*, Vol. 60, pp. 478-483, (1993).
14. Leissa, A. W., McGee, O. G., and Huang, C. S., "Vibrations of circular plates having V-notches or sharp radial cracks," *Journal of Sound and Vibration*, Vol. 161, No.2, pp. 227-239, (1993).
15. McGee, O. G., Leissa, A. W., and Huang, C. S., "Vibrations of completely free sectorial plates," *Journal of Sound and Vibration*, Vol. 164, No. 3, pp. 565-569, (1993).
16. McGee, O. G., Leissa, A. W., Huang, C. S., and Kim, J. W., "Vibrations of circular plates with clamped V-notches or rigidly constrained radial cracks," *Journal of Sound and Vibration*, Vol. 181, No. 2, pp. 185-201, (1995).
17. Williams, M. L., "Surface stress singularities resulting from various boundary conditions in angular corners of plates under bending," *Proceedings of the First U.S. National Congress of Applied Mechanics*, pp. 325-329, (1951).
18. Huang, C. S., "Singularities in plate vibration problems," Ph.D. Dissertation, The Ohio State University, Columbus, Ohio, U.S.A., (1991).